



HAL
open science

Least Squares Spherical Harmonics Approximation on the Cubed Sphere

Jean-Baptiste Bellet, Jean-Pierre Croisille

► **To cite this version:**

Jean-Baptiste Bellet, Jean-Pierre Croisille. Least Squares Spherical Harmonics Approximation on the Cubed Sphere. 2022. hal-03788836

HAL Id: hal-03788836

<https://hal.science/hal-03788836>

Preprint submitted on 27 Sep 2022

HAL is a multi-disciplinary open access archive for the deposit and dissemination of scientific research documents, whether they are published or not. The documents may come from teaching and research institutions in France or abroad, or from public or private research centers.

L'archive ouverte pluridisciplinaire **HAL**, est destinée au dépôt et à la diffusion de documents scientifiques de niveau recherche, publiés ou non, émanant des établissements d'enseignement et de recherche français ou étrangers, des laboratoires publics ou privés.

LEAST SQUARES SPHERICAL HARMONICS APPROXIMATION ON THE CUBED SPHERE

JEAN-BAPTISTE BELLET AND JEAN-PIERRE CROISILLE

ABSTRACT. The Cubed Sphere grid is an important tool to approximate functions or data on the sphere. We introduce an approximation framework on this grid based on least squares and on a suitably chosen subspace of spherical harmonics. The main claim is that for the equiangular Cubed Sphere with step size $\pi/(2N)$, a relevant spherical harmonics subspace is the one of all SH of degree less than $2N$. This choice, which matches the Nyquist's cutoff frequency along the equatorial great circle, provides an approximation problem both well-posed and well-conditioned. A series of theoretical and numerical results supporting this fact are presented.

1. INTRODUCTION

We consider the approximation of functions defined on the Cubed Sphere grid by mean of Spherical Harmonics. Suppose that $\chi \in \text{CS}_N \rightarrow y(\chi)$ is a gridfunction (a set of data) defined at the nodes χ of the Cubed Sphere CS_N . We approximate these data by a Spherical Harmonic (SH) $f \in \mathcal{Y}_D$ where $\mathcal{Y}_D = \mathbb{Y}_0 \oplus \dots \oplus \mathbb{Y}_D$ is the space of all spherical harmonics with degree less or equal than D . The standard least squares approximation problem is

$$\inf_{f \in \mathcal{Y}_D} \sum_{\chi \in \text{CS}_N} |f(\chi) - y(\chi)|^2. \quad (\text{LS})$$

Our main observation is that the choice $D = 2N - 1$ leads to a well posed and well conditioned problem. In addition, the resulting SH approximant possesses interesting accuracy properties in the maximum norm of a function known at the nodes of CS_N only. These facts are assessed theoretically and numerically hereafter.

In [4], we have introduced a particular SH subspace with good interpolating properties on the Cubed Sphere (Lagrange interpolation). This space consists of the direct sum $\mathcal{Y}_{2N-1} \oplus \mathcal{Y}'$. The second subspace \mathcal{Y}' complements \mathcal{Y}_{2N-1} . It is such that $\mathcal{Y}' \subsetneq \mathbb{Y}_{2N} \oplus \dots \oplus \mathbb{Y}_{3N}$. This interpolation framework has been in particular used in [5] to define new spherical quadrature rules of accuracy comparable to optimal ones (Lebedev rules). Here, we show that the first subspace \mathcal{Y}_{2N-1} is a suitable choice if one wants a least squares approximant instead of an interpolant.

Approximating and interpolating data on the sphere by spherical harmonics is an old and important topic. It is still widely used nowadays in many areas in physics such as numerical climatology, cosmology, gravitation, neutronic, etc. It is a central point in quantum chemistry. It is also the core point in harmonic analysis on spheres and balls since it is the three dimensional counterpart of trigonometric approximation. For fundamental and applied aspects of spherical harmonics analysis, refer to the two recent monographs [2, 6] (theory and applications). Concerning applications in geomathematics, many chapters in the reference [7] are concerned with spherical harmonics. Regarding specifically least squares, recent works include [1, 8].

The outline is as follows. In Section 2 the setup of the problem is given. A general positive weight function is included to define the least squares functional. Theoretical results are given in Section 3. These results in particular concern estimates of the condition number of the collocation matrix. Section 4 describes the attractive block structure of the collocation matrix in the case of an invariant weight. Finally, various numerical results are reported in Section 5.

Date: August 29 2022.

Key words and phrases. Cubed sphere, least squares, spherical harmonics.

2. SETUP OF THE LEAST SQUARES PROBLEM

Our notation is as follows. For any $N \geq 1$, the equiangular Cubed Sphere CS_N is the set of $\bar{N} = 6N^2 + 2$ nodes $\chi_j \in \mathbb{S}^2$, $j = 1, \dots, \bar{N}$, defined by

$$\text{CS}_N := \left\{ \frac{1}{r}(\pm 1, u, v), \frac{1}{r}(u, \pm 1, v), \frac{1}{r}(u, v, \pm 1); \right. \\ \left. r = (1 + u^2 + v^2)^{1/2}, u = \tan \frac{i\pi}{2N}, v = \tan \frac{j\pi}{2N}, -\frac{N}{2} \leq i, j \leq \frac{N}{2} \right\}.$$

Refer to [10]. For any function $g : x \in \mathbb{S}^2 \mapsto u(x) \in \mathbb{R}$, we call $g^* : \chi \in \text{CS}_N \mapsto g^*(\chi)$ the restriction of g to CS_N ,

$$g^*(\chi) = g(x), \chi \in \text{CS}_N.$$

We denote Y_n^m the Spherical Harmonic with index (n, m) in real form,

$$Y_n^m(x(\theta, \phi)) = q_n^m(\sin \theta) \cdot (\cos \theta)^{|m|} \cdot \begin{cases} \sin m\phi, & m < 0, \\ \cos m\phi, & m \geq 0. \end{cases} \quad (1)$$

In (1), q_n^m is the polynomial of degree $n - |m|$, with the parity of $n + |m|$, defined by

$$q_n^m(t) = \sqrt{\frac{(n+1/2)(n-|m|)!}{\pi(n+|m|)!}} \cdot \left(\frac{d^{|m|+n}}{dt^{|m|+n}} \frac{1}{2^n n!} (t^2 - 1)^n \right) \cdot \begin{cases} -1, & m < 0, \\ \frac{1}{\sqrt{2}}, & m = 0, \\ 1, & m > 0. \end{cases} \quad (2)$$

We note

$$\langle u, v \rangle_{L^2(\mathbb{S}^2)} = \int_{\mathbb{S}^2} u(x)v(x)d\sigma, \quad \|u\|_{L^2(\mathbb{S}^2)} = \langle u, u \rangle_{L^2(\mathbb{S}^2)}^{1/2}.$$

Any $f \in L^2(\mathbb{S}^2)$ is expressed in the Hilbert basis $(Y_n^m)_{|m| \leq n, n \in \mathbb{N}}$ as the Fourier like decomposition

$$f = \sum_{|m| \leq n} \hat{f}_n^m Y_n^m, \quad \text{with} \quad \hat{f}_n^m = \langle f, Y_n^m \rangle_{L^2(\mathbb{S}^2)}. \quad (3)$$

For any $D \geq 0$, the space $\mathcal{Y}_D = \text{Span}(Y_n^m)_{0 \leq |m| \leq n \leq D} = \bigoplus_{n=0}^D \mathbb{Y}_n$ is such that $\dim \mathcal{Y}_D = (D+1)^2$. Let $\omega_N(\chi) > 0, \chi \in \text{CS}_N$ be a given positive weight function. Let $y(\chi)$ be a set of data given at the nodes of the CS_N . The functional \mathcal{L} is defined as

$$f \mapsto \mathcal{L}(f) = \sum_{\chi \in \text{CS}_N} \omega(\chi) |f(\chi) - y(\chi)|^2. \quad (4)$$

We consider the least squares problem: find $f \in \mathcal{Y}_D$ solution of

$$\inf_{f \in \mathcal{Y}_D} \mathcal{L}(f). \quad (\text{WLS})$$

We also use the quadrature rule \mathcal{Q} associated to ω . For $f : \mathbb{S}^2 \rightarrow \mathbb{R}$, we have by

$$\mathcal{Q}(f) = \sum_{\chi \in \text{CS}_N} \omega(\chi) f(\chi) \\ = \int_{\mathbb{S}^2} f(x) d\sigma - e_N(f), \quad (5)$$

where e_N denotes the quadrature error. In the particular case where the data y are such that $y = g^*$ for a given function g , we have

$$\mathcal{L}(f) = \|f - g\|_{L^2(\mathbb{S}^2)}^2 - e_N(|f - g|^2). \quad (6)$$

For fixed values of N and D , we call the *Vandermonde matrix* of the problem the rectangular matrix A_N^D defined by

$$A_N^D = [Y_n^m(\chi)]_{\substack{\chi \in \text{CS}_N \\ |m| \leq n \leq D}} \in \mathbb{R}^{\bar{N} \times (D+1)^2}. \quad (7)$$

We define the diagonal matrix $\Omega_N \in \mathbb{R}^{\bar{N} \times \bar{N}}$ by

$$\Omega_N = \text{diag}(\omega_N(\chi))_{\chi \in \text{CS}_N} \in \mathbb{R}^{\bar{N} \times \bar{N}}. \quad (8)$$

In vector form, the problem (WLS) is expressed as

$$\inf_{\hat{f} \in \mathbb{R}^{(D+1)^2}} \|\Omega_N^{1/2} (A_N^D \hat{f} - y)\|^2, \quad (9)$$

where $y = [y(\chi_1), \dots, y(\chi_{\bar{N}})]^\top \in \mathbb{R}^{\bar{N}}$. Uniqueness for (9), or equivalently for (LS) or (WLS), is equivalent to the injectivity of A_N^D . In this case, (9) is equivalent to the linear system

$$A_N^{D\top} \Omega_N A_N^D \hat{f} = A_N^{D\top} \Omega_N y. \quad (10)$$

A natural interpretation of (10) is as follows. Consider the following analog of the Discrete Fourier Transform (DFT) of the data $y = g^*$. Here the data are defined at the nodes of CS_N instead of at the $\theta_j = 2j\pi/N \in [0, 2\pi)$, $j = 0, \dots, N$, in the standard DFT. The Fourier-like coefficients are the components of the vector

$$\begin{aligned} \text{DFT}(y) &= \left[\sum_{\chi \in \text{CS}_N} \omega(\chi) Y_n^m(\chi) y(\chi) \right]_{(n,m)} \\ &= A_N^{D\top} \Omega_N y. \end{aligned} \quad (11)$$

On the other hand, the analog of the Inverse Discrete Fourier Transform (IDFT) of a set of data $\hat{f} = [\hat{f}_n^m]_{0 \leq |m| \leq n \leq D}$ is the gridfunction

$$\begin{aligned} \text{IDFT}[\hat{f}](\chi) &= \sum_{0 \leq |m| \leq n \leq D} \hat{f}_n^m Y_n^m(\chi), \quad \chi \in \text{CS}_N, \\ &= \left[(A_N^D) \hat{f} \right](\chi). \end{aligned} \quad (12)$$

This means that in matrix form, A_N^D coincides with the IDFT operator. Therefore in terms of DFT/IDFT, the solution $f \in \mathcal{Y}_D$ of (10) has coefficients $\hat{f} = [\hat{f}_n^m]$ solution of

$$\text{DFT} \left(\text{IDFT}[\hat{f}] - y \right) = 0 \quad (13)$$

For any N , there is a maximal degree D such that the matrix A_N^D is injective (full column rank), thus guarantying that (WLS) has a unique solution. The proof consists in observing that such degrees D form a nonempty set of integers. Using that $\text{rank}(A_N^D) \leq \bar{N}$, we deduce that such D 's are bounded above by $\bar{N}^{1/2} - 1 \approx 2.45N - 1$.

Definition 1. We call D_N the maximal degree of Spherical Harmonics such that $A_N^{D_N}$ is injective.

It obviously satisfies $D_N \leq \bar{N}^{1/2} - 1$. This integer is the threshold degree such that the two following assertions hold:

- (i) For every degree $D \leq D_N$, the Vandermonde matrix A_N^D is injective. In this case (LS) has a unique solution.
- (ii) For every degree $D > D_N$, the Vandermonde matrix A_N^D is not injective. In this case (LS) has several solutions.

The rest of the paper is devoted to assess the following claim.

Claim 2. Consider the equiangular Cubed Sphere CS_N with angular stepsize $\pi/(2N)$. The maximal degree D satisfying existence/uniqueness of (WLS) **and** $\text{cond}(A_N^D)$ uniformly bounded above with respect to N is

$$D = 2N - 1. \quad (14)$$

Note that the cutoff degree $2N$ corresponds to the Nyquist angular frequency of a signal sampled with stepsize $\pi/(2N)$.

In other words, the matrix A_N^D is required to satisfy both injectivity and numerically suitable condition number. In Section 3, several theoretical results support Claim 2. However a fully theoretical proof is missing for the moment. Section 5 reports numerical results supporting Claim 2.

3. THEORETICAL RESULTS

In Section 3.1, we establish bounds for the smallest singular value as well as for the condition number of the matrix A_{2N}^{2N} . These bounds show that for $D \geq 2N$, the least squares problem is ill-posed in the case of a constant weight function (problem (LS)). This shows that, for reasons of stability of the numerical procedure, the degree D must be selected such as $D \leq 2N - 1$. Section 3.2 relates the problem (WLS) to the accuracy of the rule \mathcal{Q} in (5).

3.1. The Y_{2N}^{-2N} spherical harmonic. Consider the spherical harmonic $Y_{2N}^{-2N} \in \mathbb{Y}_{2N}$, given by, see (1)

$$Y_{2N}^{-2N}(x(\theta, \phi)) = q_{2N}^{-2N}(\sin \theta) \cdot \cos^{2N} \theta \cdot \sin(2N\phi). \quad (15)$$

By shifting the angle ϕ by $\pi/4$ we obtain $f_N \in \mathbb{Y}_{2N}$ defined by

$$f_N(x(\theta, \phi)) = Y_{2N}^{-2N}(x(\theta, \phi - \frac{\pi}{4})). \quad (16)$$

The key is to establish that f_N^* "almost vanishes" at all the Cubed Sphere nodes $\chi \in \text{CS}_N$. This will prove that when taking $D = 2N$, the Vandermonde matrix A_N^{2N} cannot be full column rank (injective) while keeping a bounded condition number. We begin with the particular case of a small Cubed Sphere with $1 \leq N \leq 4$.

Theorem 3. *For $1 \leq N \leq 4$, the function $f_N \in \mathbb{Y}_{2N}$ vanishes at all nodes of CS_N ($f^* \equiv 0$). This implies that the threshold degree D_N in Definition 1 satisfies $D_N \leq 2N - 1$.*

Proof. The spherical harmonic f_N is deduced from Y_{2N}^{-2N} by a rotation of $\pi/4$ around the pole axis. By invariance of \mathbb{Y}_{2N} by rotation, we have $f_N \in \mathbb{Y}_{2N}$. In addition, for any $N \geq 4$, it turns out that CS_N is contained in the set M_N of meridians defined by

$$M_N = \{x(\theta, \phi) : \theta \in [-\frac{\pi}{2}, \frac{\pi}{2}], \phi \equiv \frac{\pi}{4} (\frac{\pi}{2N})\}. \quad (17)$$

Along these meridians, the longitude angle ϕ is such that $2N(\phi - \frac{\pi}{4}) \equiv 0 (\pi)$, hence

$$f_N(x(\theta, \phi)) = q_{2N}^{-2N}(\sin \theta) \cdot \cos^{2N} \theta \cdot \sin(2N(\phi - \frac{\pi}{4})) = 0. \quad (18)$$

This implies that $f(\chi) = 0$ for all $\chi \in \text{CS}_N$. In particular, the linear map $f \in \mathcal{Y}_{2N} \mapsto f^*$ is not injective. Therefore, the matrix A_N^{2N} of this map is not injective. This implies in turn $D_N < 2N$. \square

Consider now the general case $N > 4$. The proof of Theorem 3 shows that the function f_N vanishes on M_N . This implies that f_N vanishes at all nodes of the four equatorial panels (I), (II), (III), (IV) of CS_N . Furthermore, f_N satisfies the estimate

$$|f_N(x(\theta, \phi))| \leq \gamma_N \cdot \cos^{2N} \theta, \quad \theta \in [-\frac{\pi}{2}, \frac{\pi}{2}], \phi \in \mathbb{R}. \quad (19)$$

The constant γ_N is

$$\gamma_N = \sqrt{\frac{4N+1}{2\pi}} \cdot \frac{\sqrt{(4N)!}}{2^{2N}(2N)!} \sim \frac{1}{\pi^{1/2}} \left(\frac{2N}{\pi}\right)^{1/4} (\approx 0.504 N^{1/4}). \quad (20)$$

(The Stirling formula has been used). Now, the behaviour of f_N on the north panel (V) and south panel (VI) is obtained by examining the nodes located outside of M_N , where the estimate (19) can be applied. Let $H_N \subset \text{CS}_N$ be the set of nodes defined by

$$H_N \triangleq \left\{ \frac{1}{r}(u, v, \pm 1) : r = (1 + u^2 + v^2)^{1/2}, u = \tan \frac{i\pi}{2N}, v = \tan \frac{j\pi}{2N}, \right. \\ \left. -\frac{N}{2} < i, j < \frac{N}{2}, |i| \neq |j| \text{ and } i \neq 0 \text{ and } j \neq 0 \right\}; \quad (21)$$

As observed in Fig. 1, we have that

$$\text{CS}_N \setminus M_N \subset H_N. \quad (22)$$

The number of nodes in H_N is given by

$$|H_N| = \begin{cases} 2(N-1)(N-3), & \text{if } N \text{ is odd,} \\ 2(N-2)(N-4), & \text{if } N \text{ is even.} \end{cases} \quad (23)$$

These observations permit to prove the following theorem

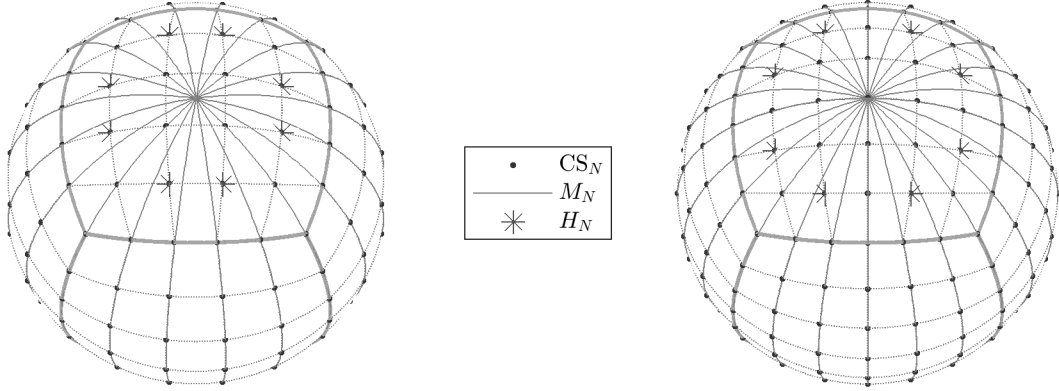


FIGURE 1. Equiangular Cubed Sphere and equiangular meridians. The Cubed Sphere CS_N (black dots) meshes \mathbb{S}^2 with equiangular arcs of great circles (dotted lines), including the radial projection of the edges of $[-1, 1]^3$ (bold gray lines). The set M_N of equiangular meridians with longitude $\phi \equiv \frac{\pi}{4} \left(\frac{\pi}{2N}\right)$ (gray lines) contains “many” points of CS_N ; the remaining points of CS_N belong to the set H_N (indicated with star symbols) defined in (21). The size of H_N is given in (23), and is estimated by $|H_N| \sim \frac{1}{3}\bar{N}$. Left panel: N is odd ($N = 5$), right panel: N is even ($N = 6$).

Theorem 4. Fix $N \geq 1$ and $D \geq 2N$.

(i) The smallest singular value of the matrix A_N^D , denoted by $\sigma_{\min}(A_N^D)$, satisfies

$$\sigma_{\min}(A_N^D)^2 \leq \gamma_N^2 \cdot |H_N| \cdot \left(\frac{2}{3}\right)^{2N} \underset{N \rightarrow +\infty}{\sim} N \left(\frac{2N}{\pi}\right)^{3/2} \left(\frac{2}{3}\right)^{2N} \underset{N \rightarrow +\infty}{\rightarrow} 0,$$

where γ_N is given by (20), and $|H_N|$ is the estimation (23) of the size of $CS_N \setminus M_N$. In particular

$$\lim_{N \rightarrow +\infty} \sigma_{\min}\left((A_N^{2N})^\top A_N^{2N}\right) = 0. \quad (24)$$

(ii) In the case where A_N^D is injective, then the condition number of A_N^D , denoted by $\text{cond}(A_N^D)$, satisfies

$$\text{cond}(A_N^D)^2 \geq \frac{\bar{N}}{|H_N|} \cdot \frac{1}{4\pi\gamma_N^2} \cdot \left(\frac{3}{2}\right)^{2N} \underset{N \rightarrow +\infty}{\sim} \frac{1}{4} \left(\frac{\pi}{2N}\right)^{1/2} \left(\frac{3}{2}\right)^{2N+1} \underset{N \rightarrow +\infty}{\rightarrow} +\infty,$$

where $\bar{N} = 6N^2 + 2$. In particular,

$$\lim_{N \rightarrow +\infty} \text{cond}\left((A_N^{2N})^\top A_N^{2N}\right) = +\infty. \quad (25)$$

Proof. (i) If $\bar{N} < (D+1)^2$, then A_N^D cannot have full column rank and the result is obvious: $\sigma_{\min}(A_N^D) = 0$. Otherwise, $\sigma_{\min}(A_N^D)^2$ is the smallest eigenvalue of the symmetric matrix $A_N^{D\top} A_N^D$ and it is the minimum Rayleigh quotient:

$$\sigma_{\min}(A_N^D)^2 = \inf_{\substack{\hat{f} \in \mathbb{R}^{(D+1)^2} \\ \|\hat{f}\|=1}} \left(\hat{f}^\top A_N^{D\top} A_N^D \hat{f} \right).$$

With the Fourier-like expansion (12), we obtain $\hat{f}^\top A_N^{D\top} A_N^D \hat{f} = \|A_N^D \hat{f}\|^2 = \sum_{\chi \in \text{CS}_N} f(\chi)^2$, so that

$$\sigma_{\min}(A_N^D)^2 = \inf_{\substack{f \in \mathcal{Y}_D \\ \|f\|_{L^2(\mathbb{S}^2)}=1}} \left(\sum_{\chi \in \text{CS}_N} f(\chi)^2 \right).$$

Let f_N be the function defined in (16); then f_N is a rotation of the unitary function $Y_{2N}^{-2N} \in \mathcal{Y}_D$, so $f_N \in \mathcal{Y}_D$ with $\langle f, f \rangle = 1$, which proves that

$$\sigma_{\min}(A_N^D)^2 \leq \sum_{\chi \in \text{CS}_N} f(\chi)^2.$$

On the right hand-side, many terms in the sum vanish. As observed in (22), $\text{CS}_N \setminus H_N \subset M_N$, where M_N and H_N are defined in (17) and (21). Thus using (18), $f(\chi) = 0$ if $\chi \in \text{CS}_N \setminus H_N$. Therefore,

$$\sigma_{\min}(A_N^D)^2 \leq \sum_{\chi \in \text{CS}_N} f(\chi)^2 = \sum_{\chi \in H_N} f(\chi)^2.$$

If H_N is empty, we obtain $\sigma_{\min}(A_N^D)^2 = 0$ and (i) is proved. Otherwise,

$$\sigma_{\min}(A_N^D)^2 \leq |H_N| \max_{\chi \in H_N} f(\chi)^2,$$

where $|H_N|$ is the cardinal number given by (23); we estimate $\max_{\chi \in H_N} f(\chi)^2$ using (19),

$$\max_{\chi \in H_N} f(\chi)^2 \leq \gamma_N^2 c^{2N}, \quad \text{with } c = \max_{\chi \in H_N} \cos^2 \theta(\chi).$$

For any $\chi = \frac{1}{(1+u^2+v^2)^{1/2}}(u, v, \pm 1) \in H_N$, with $|u|, |v| < 1$, the latitude angle $\theta(\chi)$ is such that $\cos^2 \theta(\chi) = 1 - \sin^2 \theta(\chi) = 1 - \frac{1}{1+u^2+v^2} < \frac{2}{3}$, which proves that $c < \frac{2}{3}$.

(ii) If A_N^D is injective, the condition number is the ratio

$$\text{cond}(A_N^D) = \frac{\sigma_{\max}(A_N^D)}{\sigma_{\min}(A_N^D)},$$

where $\sigma_{\min}(A_N^D)$ has been bounded in (i), and $\sigma_{\max}(A_N^D)$ denotes the largest singular value of A_N^D . The square $\sigma_{\max}(A_N^D)^2$ is the largest eigenvalue of $A_N^{D\top} A_N^D$ and it is the maximum Rayleigh ratio

$$\sigma_{\max}(A_N^D)^2 = \sup_{\substack{\hat{f} \in \mathbb{R}^{(D+1)^2} \\ \|\hat{f}\|=1}} \left(\hat{f}^\top A_N^{D\top} A_N^D \hat{f} \right) = \sup_{\substack{f \in \mathcal{Y}_D \\ \|f\|_{L^2(\mathbb{S}^2)}=1}} \sum_{\chi \in \text{CS}_N} f(\chi)^2.$$

With $f(x) = Y_0^0(x) = \frac{1}{\sqrt{4\pi}}$ we obtain the lower bound $\sigma_{\max}(A_N^D)^2 \geq \frac{\bar{N}}{4\pi}$. \square

3.2. Least squares and quadrature rule accuracy. Proving the well posedness of (WLS) amounts to establish bounds for the condition number of the matrix $A_N^{D\top} \Omega_N A_N^D$. We have

$$A_N^{D\top} \Omega_N A_N^D = \left[\sum_{\chi \in \text{CS}_N} \omega_N(\chi) Y_n^m(\chi) Y_{n'}^{m'}(\chi) \right]_{\substack{|m| \leq n \leq D \\ |m'| \leq n' \leq D}} \in \mathbb{R}^{(D+1)^2 \times (D+1)^2}. \quad (26)$$

This matrix contains inner products involving the grid functions $(Y_n^m)^*$, for the discrete weighted inner product defined by

$$(y_1, y_2)_{\omega_N} \triangleq \sum_{\chi \in \text{CS}_N} \omega_N(\chi) y_1(\chi) y_2(\chi), \quad y_1, y_2 : \text{CS}_N \rightarrow \mathbb{R}. \quad (27)$$

The functions Y_n^m are orthonormal for the inner product $\langle \cdot, \cdot \rangle_{L^2(\mathbb{S}^2)}$. However, for the discrete product $(\cdot, \cdot)_{\omega_N}$, we only have $(Y_n^m, Y_{n'}^{m'})_{\omega_N} \approx 0$.

Theorem 5. Fix $N \geq 1$ and $D \geq 0$. Let A_N^D be the Vandermonde matrix with degree D on CS_N , defined in (7). Let $\omega_N : \text{CS}_N \rightarrow (0, \infty)$ be the weight of a spherical quadrature rule on CS_N , with error e_N ; let Ω_N be the associated diagonal matrix, defined in (8). Then

$$A_N^{D\top} \Omega_N A_N^D = \mathbf{I}_{(D+1)^2} - E_N^D, \quad (28)$$

where E_N^D is a symmetric matrix containing the quadrature errors:

$$E_N^D = \left[e_N(Y_n^m Y_{n'}^{m'}) \right]_{\substack{|m| \leq n \leq D \\ |m'| \leq n' \leq D}} \in \mathbb{R}^{(D+1)^2 \times (D+1)^2}. \quad (29)$$

In particular, assume that $(\omega_N)_{N \geq 1}$ defines a convergent spherical quadrature rule on \mathcal{Y}_{2D} , i.e. $\forall f \in \mathcal{Y}_{2D}$, $e_N(f) \xrightarrow{N \rightarrow \infty} 0$, then

$$A_N^{D\top} \Omega_N A_N^D \xrightarrow{N \rightarrow \infty} \mathbf{I}_{(D+1)^2};$$

moreover, if the rule converges with order $p > 0$, i.e. $\forall f \in \mathcal{Y}_{2D}$, $\exists C_f \geq 0$, $\forall N \geq 1$, $|e_N(f)| \leq C_f N^{-p}$, then

$$A_N^{D\top} \Omega_N A_N^D = \mathbf{I}_{(D+1)^2} + \mathcal{O}\left(\frac{1}{N^p}\right).$$

The relation (28) expresses the fact that the matrix $A_N^{D\top} \Omega_N A_N^D$ is close to the identity, assuming that the error matrix entries are small. This is the case when ω_N defines an accurate quadrature rule on the space \mathcal{Y}_{2D} . This will require that D is not too large compared to N . On the contrary, for large values of D , the entries in E_N^D are not a priori small.

Proof. In the matrix $A_N^{D\top} \Omega_N A_N^D$, the entry with row index (n, m) and column index (n', m') contains the discrete inner product $((Y_n^m)^*, (Y_{n'}^{m'})^*)_{\omega_N}$, as described in (26) and (27). Using the quadrature rule (5) with $g = Y_n^m Y_{n'}^{m'}$ shows that this element is expressed as

$$((Y_n^m)^*, (Y_{n'}^{m'})^*)_{\omega_N} = \int_{\mathbb{S}^2} Y_n^m(x) Y_{n'}^{m'}(x) d\sigma - e_N(Y_n^m Y_{n'}^{m'}).$$

Since the functions Y_n^m are orthonormal in $L^2(\mathbb{S}^2)$, we have

$$\int_{\mathbb{S}^2} Y_n^m(x) Y_{n'}^{m'}(x) d\sigma = \langle Y_n^m, Y_{n'}^{m'} \rangle_{L^2(\mathbb{S}^2)} = \begin{cases} 1, & \text{if } (n, m) = (n', m'), \\ 0, & \text{otherwise.} \end{cases}$$

This proves (28). The symmetry of E_N^D is obvious.

Finally for a convergent rule, for all $|m| \leq n \leq D$ and $|m'| \leq n' \leq D$, the entry of E_N^D with indices (n, m) and (n', m') is related to $f = Y_n^m Y_{n'}^{m'} \in \mathcal{Y}_{2D}$, so that by hypothesis $e_N(Y_n^m Y_{n'}^{m'}) \rightarrow 0$. For a convergence of order $p > 0$, there is furthermore a constant $C_{n,m}^{m',m'}$ such that $|e_N(Y_n^m Y_{n'}^{m'})| \leq C_{n,m}^{m',m'} N^{-p}$. \square

4. BLOCK STRUCTURE OF $(A_N^D)^\top \Omega_N A_N^D$ FOR A SYMMETRIC WEIGHT FUNCTION

The weight function $\chi \in \text{CS}_N \mapsto w(\chi)$ plays the role of a parameter in the problem (WLS). Here we consider the important case of a weight $w(\chi)$ with cubic symmetry. This property has been considered in [5, 9].

Theorem 6. Assume that $\omega_N : \text{CS}_N \rightarrow (0, \infty)$ is invariant under the symmetry group \mathcal{G} of the cube $\{-1, 1\}^3$. Consider a nonzero entry $e_N(Y_n^m Y_{n'}^{m'})$ of the symmetric matrix E_N^D defined in (29), with row index (n, m) , and column index (n', m') . Then the four following conditions hold

- (i) $n \equiv n' \pmod{2}$ (same parity for the degrees);
- (ii) $m, m' \geq 0$, or $m, m' < 0$ (same sign for the orders);
- (iii) $m \equiv m' \pmod{2}$ (same parity for the orders);
- (iv) if $m, m' \equiv 0 \pmod{2}$, then $m \equiv m' \pmod{4}$.

Proof. The proof principle is close to the one of [5, Corollary 10]. To begin with, [3] proves that the group \mathcal{G} of the cube, described by

$$\mathcal{G} = \left\{ \left[\begin{array}{ccc} \epsilon_1 e_{\sigma_1} & \epsilon_2 e_{\sigma_2} & \epsilon_3 e_{\sigma_3} \end{array} \right], \sigma \in \mathfrak{S}_3, \epsilon \in \{-1, 1\}^3 \right\}, \quad e_1 = (1, 0, 0), \quad e_2 = (0, 1, 0), \quad e_3 = (0, 0, 1), \quad (30)$$

is also the symmetry group of CS_N . Therefore, the quadrature error defines a linear form

$$e_N : \mathcal{Y}_{2D} \rightarrow \mathbb{R}, \quad e_N(g) = \int_{\mathbb{S}^2} g(x) \, d\sigma - \sum_{\chi \in \text{CS}_N} \omega_N(\chi) g(\chi),$$

which is invariant under \mathcal{G} , *i.e.* $\forall Q \in \mathcal{G}, e_N(g(Q^\top \cdot)) = e_N(g)$.

In the sequel, for all (n, m) and (n', m') violating at least one of the conditions (i)-(iv), we consider $g = Y_n^m Y_{n'}^{m'} \in \mathcal{Y}_{2D}$, and we exhibit a matrix $Q \in \mathcal{G}$ such that $g(Q^\top x) = -g(x)$. This is a sufficient condition to ensure that $e_N(g) = 0$, due to $e_N(g) = e_N(g(Q^\top \cdot)) = e_N(-g) = -e_N(g)$. The proof is a calculation in spherical coordinates, based on the expression

$$\begin{aligned} g(x(\theta, \phi)) &= (q_n^m q_{n'}^{m'}) (\sin \theta) \cdot \cos^{|m|} \theta \cos^{|m'|} \theta \\ &\quad \cdot (\sin(m\phi) \mathbf{1}_{m < 0} + \cos(m\phi) \mathbf{1}_{m \geq 0}) (\sin(m'\phi) \mathbf{1}_{m' < 0} + \cos(m'\phi) \mathbf{1}_{m' \geq 0}). \end{aligned}$$

Case 1: (ii) is violated. Assume $m < 0$ and $m' \geq 0$ (without loss of generality), then

$$g(Q^\top x(\theta, \phi)) = g(x(\theta, -\phi)) = -g(x(\theta, \phi)), \quad \text{for } Q := \begin{bmatrix} 1 & 0 & 0 \\ 0 & -1 & 0 \\ 0 & 0 & 1 \end{bmatrix}.$$

Case 2: (iii) is violated. Assume that $m \equiv 1 \pmod{2}$ and $m' \equiv 0 \pmod{2}$ (without loss of generality). Then $m(\phi + \pi) \equiv m\phi + \pi \pmod{2\pi}$, $m'(\phi + \pi) \equiv m'\phi \pmod{2\pi}$, and

$$g(Q^\top x(\theta, \phi)) = g(x(\theta, \phi + \pi)) = -g(x(\theta, \phi)), \quad \text{for } Q := \begin{bmatrix} -1 & 0 & 0 \\ 0 & -1 & 0 \\ 0 & 0 & 1 \end{bmatrix}.$$

Case 3: (iii) is satisfied but (i) is violated. Assume that $n + |m| \equiv 1 \pmod{2}$ and $n' + |m'| \equiv 0 \pmod{2}$ (without loss of generality). Then $\theta \mapsto (q_n^m q_{n'}^{m'}) (\sin \theta)$ is odd, hence

$$g(Q^\top x(\theta, \phi)) = g(x(-\theta, \phi)) = -g(x(\theta, \phi)), \quad \text{for } Q := \begin{bmatrix} 1 & 0 & 0 \\ 0 & 1 & 0 \\ 0 & 0 & -1 \end{bmatrix}.$$

Case 4: (iv) is violated. Assume that $m \equiv 2 \pmod{4}$ and $m' \equiv 0 \pmod{4}$ (without loss of generality). Then $m(\phi + \frac{\pi}{2}) \equiv m\phi + \pi \pmod{2\pi}$, $m'(\phi + \frac{\pi}{2}) \equiv m'\phi \pmod{2\pi}$, and

$$g(Q^\top x(\theta, \phi)) = g(x(\theta, \phi + \frac{\pi}{2})) = -g(x(\theta, \phi)), \quad \text{for } Q := \begin{bmatrix} 0 & 1 & 0 \\ -1 & 0 & 0 \\ 0 & 0 & 1 \end{bmatrix}. \quad \square$$

Roughly speaking, if the weight ω_N is symmetric, then a minimal ratio of

$$\frac{3}{32} = 9.375\% \quad (31)$$

of all the entries in E_N^D are nonzero. Indeed, Case (i) divides by 2 the number of possible nonzero entries. Then Case (ii) further divides by 2 this number. And finally Cases (iii-iv) multiply this number by $\frac{3}{8}$. Then, two facts suggest the approximation

$$A_N^{D\top} \Omega_N A_N^D \approx \mathbf{I}_{(D+1)^2} :$$

- as much as $\approx \frac{29}{32}$ of all entries are identical if ω_N is assumed symmetric (Theorem 6);
- the remaining entries ($\approx \frac{3}{32}$) are small assuming that ω_N defines an accurate spherical quadrature rule in \mathcal{Y}_{2D} , (see Theorem 5).

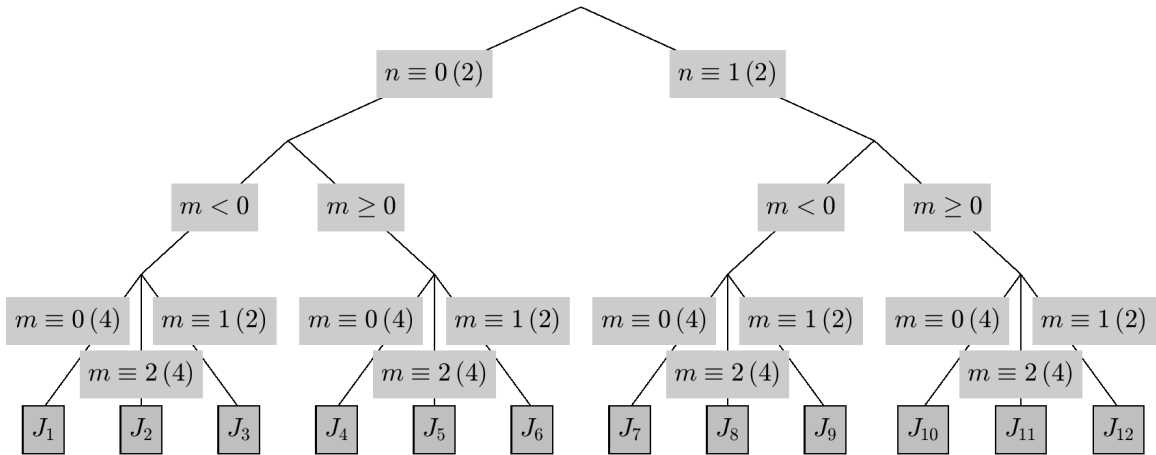


FIGURE 2. Classification tree for partitioning the set of indices $\{(n, m) : |m| \leq n \leq D\}$ as a disjoint union $J_1 \sqcup \dots \sqcup J_{12}$; for instance, $J_4 = \{|m| \leq n \leq D, n \equiv 0(2), m \geq 0, m \equiv 0(4)\}$.

In particular, the condition number of the matrix $A_N^{D\top} \Omega_N A_N^D$ is expected to be close to 1, so that (WLS) is expected to be well-posed. This point is further investigated numerically in Section 5.3.

Next, we go one step further in the analysis taking benefit from the orthogonality relations in Theorem 6. Indeed, Theorem 6 suggests to sort the indices (n, m) using the following criteria, ordered by decreasing priority:

- case $n \equiv 0(2)$ and case $n \equiv 1(2)$;
- case $m < 0$ and case $m \geq 0$;
- case $m \equiv 0(4)$, then case $m \equiv 2(4)$, and finally case $m \equiv 1(2)$.

This particular ordering partitions the set of indices as a disjoint union of the twelve sets J_k , $1 \leq k \leq 12$. They are displayed in the classification tree of Figure 2; it permits to express the orthogonality relations in Theorem 6 as follows.

Corollary 7. Fix $N \geq 1$, $D \geq 0$, and $\omega_N : \text{CS}_N \rightarrow (0, \infty)$ invariant under the group \mathcal{G} of $\{-1, 1\}^3$. Let J_k , $1 \leq k \leq 12$, denotes a partitioning of the set of indices $|m| \leq n \leq D$, as in Figure 2.

- (i) Assume that the indices $(n, m) \in J_k$, $1 \leq k \leq 12$ in the Vandermonde matrix A_N^D are sorted along increasing k (for the rows and for the columns). Then $A_N^{D\top} \Omega_N A_N^D$ is block diagonal, as shown in Figure 3.
- (ii) The following orthogonal decomposition holds for the discrete inner product (27),

$$\{f^*, f \in \mathcal{Y}_D\} = \bigoplus_{k=1}^{12} \text{Span}\{(Y_n^m)^*, (n, m) \in J_k\}.$$

Assuming a symmetrical weight, Corollary 7 reveals that the matrix $A_N^{D\top} \Omega_N A_N^D$, associated to (WLS), is block diagonal, for a particular ordering of the indices. This has the following consequence to solve the system (10). Instead of solving a linear system with $(D+1)^2$ unknowns, the system is solved by blocks. It consists in solving eight square linear systems with $\approx \frac{1}{16}(D+1)^2$ unknowns, and four square linear systems with $\approx \frac{1}{8}(D+1)^2$ unknowns. These resolutions can be obviously performed in parallel.

Remark 8. In [3, Corollary 10], the “15/16” property is coined as meaning exactness of a symmetric quadrature rule for a certain proportion of 15/16 of all spherical harmonics. This property can be deduced from Corollary 7. Indeed, consider a symmetric weight ω_N , a row index $(n, m) \notin J_4$,

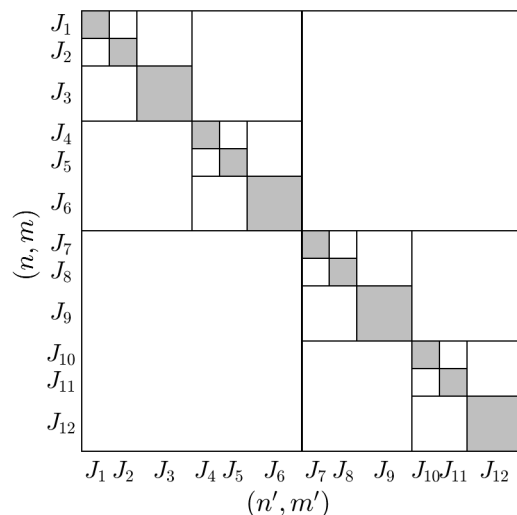


FIGURE 3. Block diagonal structure of the matrix $A_N^{D\top} \Omega_N A_N^D$, assuming that ω_N is invariant under \mathcal{G} ; the sets of indices J_k are defined in Figure 2. The white cells contains only null coefficients; they represent about $\frac{29}{32}$ of the entries.

and the column index $(n', m') = (0, 0) \in J_4$; then $Y_n^{m'} \equiv (4\pi)^{-1/2}$, and we deduce from Corollary 7.(i) that

$$\mathcal{Q}(Y_n^m) = \sum_{\chi \in \text{CS}_N} \omega_N(\chi) Y_n^m(x) = 0 = \int_{\mathbb{S}^2} Y_n^m(x) d\sigma.$$

Since J_4 contains about 1/16 of the indices, we see that the quadrature rule \mathcal{Q} associated to ω_N integrates exactly about 15/16 of the Y_n^m .

5. NUMERICAL RESULTS

5.1. Condition number of the Vandermonde matrix. We assess numerically that (LS) is well-posed for the degree $D = 2N - 1$, but not for $D = 2N$.

For that purpose, for every $1 \leq N \leq 32$, for $D = 2N - 1, 2N$, we first compute a singular value decomposition of the Vandermonde matrix A_N^D . Second, we extract the minimal singular value $\sigma_{\min}(A_N^D)$ and the maximal one $\sigma_{\max}(A_N^D)$. Finally, we deduce the condition number $\text{cond}(A_N^D) = \sigma_{\max}(A_N^D)/\sigma_{\min}(A_N^D)$. The computation have been performed in double precision in `Matlab`, using the `svd` function. The results shown in Figure 4 are as follows.

- (1) For $D = 2N - 1$ (left panel in Figure 4), we observe that the minimal singular value is “far” from 0, and that the condition number is close to 1; more precisely, the numerical values indicate that $\text{cond}(A_N^{2N-1}) \approx 1.19$. As a consequence, A_N^{2N-1} is injective. This means that the critical degree D_N insuring injectivity satisfies $D_N \geq 2N - 1$. Furthermore, $\text{cond}(A_N^{D\top} A_N^D) = \text{cond}(A_N^D)^2 \approx 1.41$, which implies that (LS) is well-posed for $D = 2N - 1$.
- (2) For $D = 2N$ (right panel in Figure 4), we observe that the minimal singular value is very close to 0 for $N \in \{1, 2, 3, 4, 5, 7, 9\}$ (the machine epsilon is about $2.2 \cdot 10^{-16}$); otherwise, it is positive and decays to 0 when N increases. Hence, for $N \in \{1, 2, 3, 4, 5, 7, 9\}$, A_N^{2N} is not injective, *i.e.* $D_N \leq 2N - 1$. This is consistent with Theorem 3 which proves this result for $N \leq 4$. This observation, combined with the discussion above, supports the fact that

$$D_N = 2N - 1, \quad N \in \{1, 2, 3, 4, 5, 7, 9\}.$$

For the other values of N , it appears that A_N^{2N} is injective, so that $D_N \geq 2N$. Nevertheless, for these values of N , $\text{cond}(A_N^{2N-1}) > 10^4$, and blows-up when N increases. Consequently $\text{cond}(A_N^{2N\top} A_N^{2N}) > 10^8$ and blows-up when N increases. Therefore, for

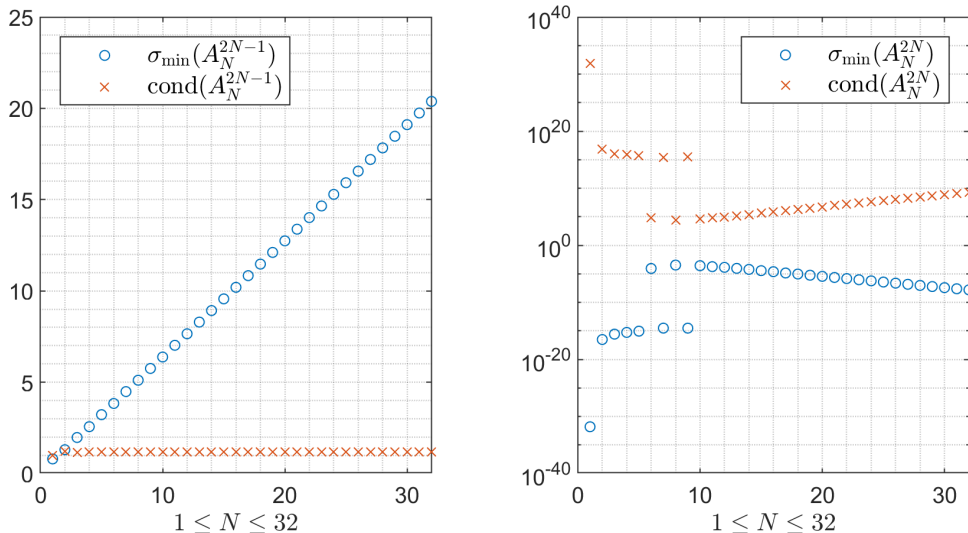


FIGURE 4. Smallest singular value (σ_{\min}) and condition number (cond) of Vandermonde matrices A_N^D , $1 \leq N \leq 32$, with $D = 2N - 1$ (left), and $D = 2N$ (right, in log-scale). Left panel: A_N^{2N-1} is injective ($\sigma_{\min} \gg 0$) and very well-conditioned ($\text{cond} \approx 1.19$). Right panel: A_N^{2N} is not injective if N is small ($\sigma_{\min} \approx 0$), and is ill-conditioned otherwise ($\text{cond} > 10^4$).

i	$f_i(x, y, z)$	Comment
1	$\exp(x)$	Very smooth
2	$\frac{3}{4} \exp\left[-\frac{(9x-2)^2}{4} - \frac{(9y-2)^2}{4} - \frac{(9z-2)^2}{4}\right]$ $+\frac{3}{4} \exp\left[-\frac{(9x+1)^2}{49} - \frac{9y+1}{10} - \frac{9z+1}{10}\right]$ $+\frac{1}{2} \exp\left[-\frac{(9x-7)^2}{4} - \frac{(9y-3)^2}{4} - \frac{(9z-5)^2}{4}\right]$ $-\frac{1}{5} \exp[-(9x-4)^2 - (9y-7)^2 - (9z-5)^2]$	Smooth
3	$\frac{1}{10} \frac{\exp(x+2y+3z)}{(x^2+y^2+(z+1)^2)^{1/2}} \mathbf{1}(z > -1)$	Infinite spike at the south pole ($z = -1$)
4	$\cos(3 \arccos z) \mathbf{1}(3 \arccos z \leq \frac{\pi}{2})$	Continuous, not differentiable ($z = \frac{\sqrt{3}}{2}$)
5	$\mathbf{1}(z \geq \frac{1}{2})$	Discontinuous spherical cap ($z = \frac{1}{2}$)

TABLE 1. A series of test functions representative of various regularity properties.

$D = 2N$, (LS) is ill-posed even if A_N^{2N} is injective, and the ill-posedness level increases with N .

The numerical study presented here suggests that for any $N \geq 1$, the maximal degree guaranteeing well posedness and well conditioning is $D = 2N - 1$. This implies that any $f \in \mathcal{Y}_{2N-1}$ is correctly sampled on the Cubed Sphere CS_N with angular step $\frac{\pi}{2N}$, since (LS) can reconstruct f from f^* in a stable way. If $f \in \mathcal{Y}_D$ with $D \geq 2N$, this property is not guaranteed.

5.2. Accuracy of the least squares approximation. We compute least-squares approximations of test functions, without and with noise. We follow the recommendation of Subsection 5.1: for the grid CS_N , we work in the approximation space \mathcal{Y}_{2N-1} , since it is the largest approximation space \mathcal{Y}_D ensuring well-posedness for (LS).

First, we report in Table 1 five test functions in [3] (and the references therein); this series of functions is representative of various regularity properties. For each $1 \leq N \leq 32$ and for each test function f_i , $1 \leq i \leq 5$, we compute the least-squares approximation $\tilde{f}_i \in \mathcal{Y}_{2N-1}$ of f_i from the grid function $(f_i)^*$: \tilde{f}_i is evaluated as the unique solution to (LS), for $D = 2N - 1$ and $y = (f_i)^*$. The accuracy is measured by the relative discrete error, on a reference fine grid CS_M

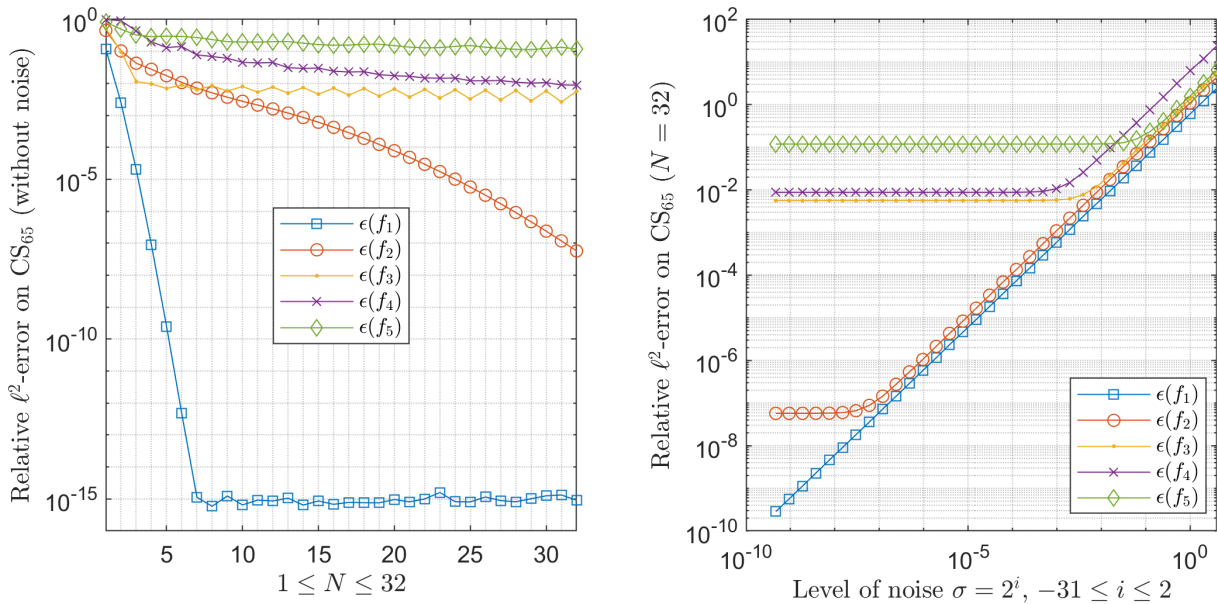


FIGURE 5. Least-squares approximation (LS) of the test functions f_i from Table 1. Left panel: for any $1 \leq N \leq 32$, the approximation $\tilde{f}_i \in \mathcal{Y}_{2N-1}$ is computed from $(f_i)^*$, and the relative ℓ^2 -error $\epsilon(f_i)$ defined in (32) is plotted. Right panel: for any level of noise $\sigma = 2^j$, $-31 \leq j \leq 2$, the approximation $\tilde{f}_i \in \mathcal{Y}_{63}$ is computed from a noisy dataset $(f_i)^* + \sigma\mathcal{N}(0, 1)$ with $N = 32$, and $\epsilon(f_i)$ is plotted.

defined by

$$\epsilon(f_i) := \left(\frac{\sum_{\chi \in \text{CS}_M} |f_i(\chi) - \tilde{f}_i(\chi)|^2}{\sum_{\chi \in \text{CS}_M} |f_i(\chi)|^2} \right)^{1/2}, \quad M = 65. \quad (32)$$

The errors are displayed in Fig. 5 (left panel). For the smooth functions f_1 and f_2 , the error rapidly converges to 0 when N increases; this is especially true for f_1 . For the continuous but not differentiable function f_4 , the convergence is slow. For the spike function f_3 and the discontinuous function f_5 , the convergence cannot be claimed from the plot. These observations are not surprising: it is expected that the convergence rate depends on the decay of the Fourier coefficients, which is related to the smoothness.

Second, fix the grid resolution to $N = 32$. For each test function f_i , $1 \leq i \leq 5$, for any $\sigma = 2^j$, $-31 \leq j \leq 2$, we corrupt the grid function $(f_i)^*$ with a gaussian noise with zero mean, and standard deviation σ . We compute an approximation $\tilde{f}_i \in \mathcal{Y}_{63}$ of f_i as the unique solution to (LS), for $D = 2N - 1$ and $y(\chi) = f_i(\chi) + \sigma u(\chi)$, $\chi \in \text{CS}_{32}$, where $[u(\chi)]$ contains independent realizations of the normal law $\mathcal{N}(0, 1)$. Here again, we evaluate the accuracy of this approximation by the relative error (32); this error depends on σ (and on the experiment), and we denote it by $\epsilon(f_i)(\sigma)$. These errors are displayed in Figure 5 (right panel). One observes that

$$\epsilon(f_i)(\sigma) \approx \epsilon(f_i)(0) + \sigma,$$

where $\epsilon(f_i)(0)$ is the error without noise for $N = 32$ (displayed on the left panel). In other words, a level of noise σ in the dataset increases the error by σ . This reveals that approximating a function by least-squares on CS_N in the space \mathcal{Y}_{2N-1} is very stable.

Third, we show numerically that differentiating the least-squares approximation (LS) in \mathcal{Y}_{2N-1} ($D = 2N - 1$) permits to approximate derivatives. Assume that f is a differentiable function on \mathbb{S}^2 , known by the grid function f^* . The least squares approximation (LS) of f is

$$\tilde{f} = \sum_{|m| \leq n \leq 2N-1} \tilde{f}_n^m Y_n^m \in \mathcal{Y}_{2N-1}, \quad (33)$$

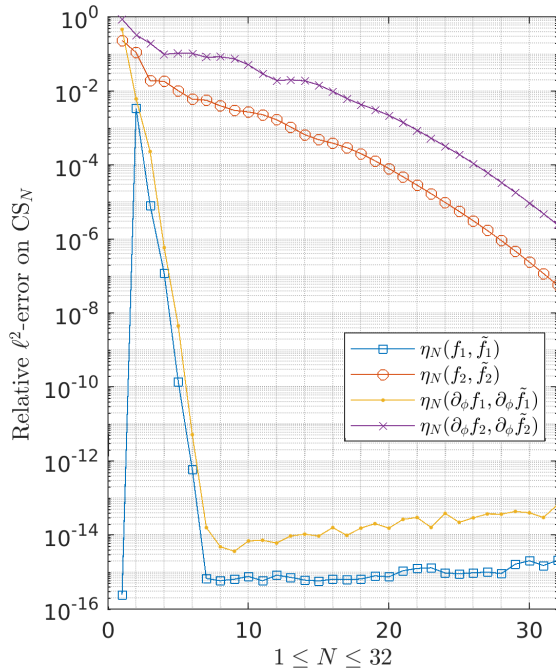


FIGURE 6. Spectral differentiation on CS_N with respect to the longitude ϕ . For $f = f_1, f_2$ from Table 1, for any $1 \leq N \leq 32$, the approximate derivative $\partial_\phi \tilde{f}$ is computed from the least-squares approximation $\tilde{f} \in \mathcal{Y}_{2N-1}$. Relative ℓ^2 -errors defined in (35) are plotted.

with $D = 2N - 1$ and $y = f^*$. Consider for instance the derivative with respect to the longitude ϕ ,

$$\partial_\phi \tilde{f}(x(\theta, \phi)) = \sum_{|m| \leq n \leq 2N-1} m \cdot \tilde{f}_n^{-m} Y_n^m(x(\theta, \phi)) \in \mathcal{Y}_{2N-1}. \quad (34)$$

We test this principle on the smooth functions defined in Table 1: $f = f_1, f_2$. For each value of $1 \leq N \leq 32$, we approximate $\partial_\phi f$ by $\partial_\phi \tilde{f}$ satisfying (34), and we calculate the relative ℓ^2 -errors on the grid CS_N :

$$\eta_N(f, \tilde{f}) = \left(\frac{\sum_{x \in CS_N} |f(x) - \tilde{f}(x)|^2}{\sum_{x \in CS_N} |f(x)|^2} \right)^{1/2}, \quad \eta_N(\partial_\phi f, \partial_\phi \tilde{f}) = \left(\frac{\sum_{x \in CS_N} |\partial_\phi f(x) - \partial_\phi \tilde{f}(x)|^2}{\sum_{x \in CS_N} |\partial_\phi f(x)|^2} \right)^{1/2}; \quad (35)$$

here, the exact derivative is given by

$$\partial_\phi f(x(\theta, \phi)) = -x_2(\theta, \phi) \partial_{x_1} f(x(\theta, \phi)) + x_1(\theta, \phi) \partial_{x_2} f(x(\theta, \phi)),$$

where $x_1(\theta, \phi)$ and $x_2(\theta, \phi)$ denote the horizontal coordinates of $x(\theta, \phi)$. As can be observed in Figure 6, the error for the derivative and the error for the function itself have a similar behavior in term of N . The least squares approximation converges to the exact function and the spectral derivative converges to the exact derivative; the observed convergence rates are similar.

5.3. Pseudo-orthogonality for the discrete inner product. We evaluate numerically the relation (28); it represents some “pseudo-orthogonality” of the Legendre basis, for the discrete inner product (27).

First, we consider the uniform quadrature rule on CS_N , defined by $\omega_N(x) = 4\pi/\bar{N}$. In this case, the matrix $A_N^{D\top} \Omega_N A_N^D$ in (10) is expressed as

$$A_N^{D\top} \Omega_N A_N^D = \frac{4\pi}{\bar{N}} A_N^{D\top} A_N^D.$$

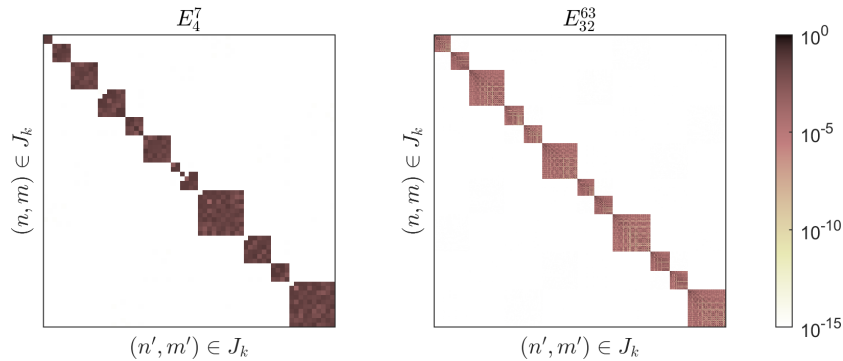


FIGURE 7. Matrix $E_N^D = [e_N(Y_n^m Y_{n'}^{m'})]$ from (28)-(29), with the uniform weight $\omega_N = 4\pi/\bar{N}$, $D = 2N - 1$, $N = 4$ (left panel) and $N = 32$ (right panel). The indices are arranged by the classification tree of Figure 2. The displayed value is $10^{-15} + |e_N(Y_n^m Y_{n'}^{m'})|$, in logarithmic scale. The observed structure is the block diagonal structure predicted by Figure 3 (Corollary 7). The sparsity score is 9.961% (left panel), resp. 9.387% (right panel), which is close to $3/32$.

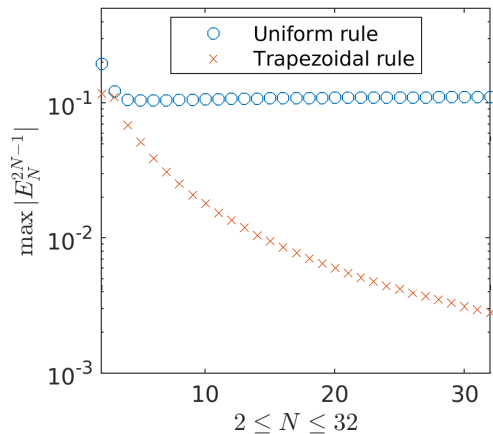


FIGURE 8. Maximal entry $\max |e_N(Y_n^m Y_{n'}^{m'})|$ of the matrix E_N^{2N-1} , $2 \leq N \leq 32$. The result depends on the accuracy of the quadrature rule ω_N , so it is smaller for the trapezoidal weight than for the uniform weight.

The uniform weight is invariant under \mathcal{G} . Thus Theorem 6 predicting a sparse structure of $E_N^D = \mathbf{I}_{(D+1)^2} - A_N^{D\top} \Omega_N A_N^D$ can be applied. More precisely, Corollary 7 predicts that E_N^D has the block diagonal structure in Figure 3, for a suitable ordering of the indices. Figure 7 reports this structure, where E_N^D is displayed with $D = 2N - 1$, for $N = 4$ and $N = 32$. In these matrices, the percentage of coefficients above 10^{-14} is respectively 9.961% and 9.387%, which is close to the ratio (31). Furthermore, we compute the largest entry of E_N^{2N-1} for $1 \leq N \leq 32$. As displayed in Figure 8, this value is about 0.1 (except for $N = 1$, for which the observed value is the machine epsilon). Therefore, the matrix corresponding to (LS) (without weight) is close to be proportional to the identity matrix.

$$A_N^{2N-1\top} A_N^{2N-1} \approx \frac{\bar{N}}{4\pi} (\mathbf{I}_{4N^2} \pm 0.1).$$

Second, we consider the weight of the trapezoidal rule in the Definition 3.1 in [9]. It is invariant under \mathcal{G} , so E_N^D has a sparse structure as before. This rule is second order accurate; so it is more accurate than the uniform one, and the entries of E_N^D are expected to be smaller, due to Theorem 5. This is confirmed in Figure 8; the maximal entry of E_N^{2N-1} is below 0.1, and it decays to zero when N increases.

6. CONCLUSION

This paper considers (weighted) least-squares approximation by spherical harmonics on the equiangular Cubed Sphere CS_N . From a theoretical point of view, the symmetric positive semi-definite matrix of the normal equations is expected to be a perturbation of the identity matrix; the magnitude of the perturbation depends on the accuracy of the quadrature rule associated to the weight. This indicates that the Legendre spherical harmonics should be almost orthogonal for some discrete inner product on CS_N . In the case of a symmetrical weight, the matrix is block diagonal; this structure directly provides subspaces of spherical harmonics which are exactly orthogonal for the discrete inner product, disregarding the magnitude of the perturbation.

From a numerical point of view, the matrix has a condition number close to 1 if the cutoff (angular) frequency is fixed to $2N - 1$, whereas it is not anymore the case if higher frequencies are considered. Numerical results indicate that \mathcal{Y}_{2N-1} is a suitable approximation space for fitting or differentiating a smooth function from values on CS_N .

Future work includes further mathematical analysis on the one hand. On the other hand, the block structure and the well conditioning of the matrix shown in Section 4 opens the way to a parallel Conjugate Gradient solver. This is a preliminary step before to investigate a genuine fast solver.

REFERENCES

- [1] C. An, X. Chen, I.H. Sloan, and R.S. Womersley. Regularized least squares approximations on the sphere using spherical designs. *SIAM J. Numer. Anal.*, 50(3):1513–1534, 2012.
- [2] K. Atkinson and W. Han. *Spherical Harmonics and Approximations on the Unit Sphere: an introduction*. Number 2044 in Lect. Notes. Math. Springer-Verlag, 2012.
- [3] J.-B. Bellet. Symmetry group of the equiangular cubed sphere. *Quart. of App. Math.*, 80:69–86, 2022.
- [4] J.-B. Bellet, M. Brachet, and J.-P. Croisille. Interpolation on the Cubed Sphere with Spherical Harmonics. 2021, submitted.
- [5] J.-B. Bellet, M. Brachet, and J.-P. Croisille. Quadrature and symmetry on the Cubed Sphere. *Jour. Comp. App. Math.*, 409(114142), 2022.
- [6] F. Dai and Y. Xu. *Approximation theory and harmonic analysis on spheres and balls*. Springer Monographs in Mathematics. Springer-Verlag, 2013.
- [7] W. Freeden, M. Z. Nashed, and T. Sonar. *Handbook of Geomathematics*. Springer, 2010.
- [8] K. Hesse and Q. T. L. Gia. L^2 error estimates for polynomial discrete penalized least-squares approximation on the sphere from noisy data. *Jour. Comp. App. Math.*, 408(114118), 2022.
- [9] B. Portelenelle and J.-P. Croisille. An efficient quadrature rule on the Cubed Sphere. *J. Comp. App. Math.*, 328:59–74, 2018.
- [10] C. Ronchi, R. Iacono, and P. S. Paolucci. The Cubed Sphere: A new method for the solution of partial differential equations in spherical geometry. *J. Comput. Phys.*, 124:93–114, 1996.

UNIVERSITÉ DE LORRAINE, CNRS, IECL, F-57000 METZ, FRANCE

Email address: jean-baptiste.bellet@univ-lorraine.fr, jean-pierre.croisille@univ-lorraine.fr